



Improving the performance parameters of organic field-effect transistors via alkyl chain length of boronic acid self-assembled monolayers

Tuğbahan Yılmaz^{1,*}

¹ Department of Electric and Energy, Konya Technical University, 42075 Konya, Turkey

Received: 7 February 2024

Accepted: 5 May 2024

Published online:
15 May 2024

© The Author(s), 2024

ABSTRACT

Interface modification is a promising technique for enhancing electrical parameters of Organic Field Effect Transistor (OFETs). In OFETs, self-assembled monolayer molecules are widely used for treatment dielectric/semiconductor interface layer. Modification of dielectric/semiconductor layer with SAM molecules ensures a variety of potential applications. Boronic acids with four different alkyl chain lengths (C_n -BA; $n = 8, 10, 12, 14$) molecules were used in this study to treat the Al_2O_3 dielectric surface in dinaphtho[2,3-b:2',3'-f]thieno[3,2-b]thiophene (DNNT) based OFETs. Treated with SAMs improve the mobility of Al_2O_3 surfaces for linear and saturation regime and threshold voltages shifted from positive direction. The morphological and electrical characterizations were performed for fabricated OFET. The results show that alkyl-boronic acids SAM molecules open a new perspective for further optoelectronic applications due to its application for oxide surfaces and controllability.

1 Introduction

Organic field effect transistors (OFETs) have great attention in future electronic applications including sensors, radio-frequency identification tags, and flexible displays due to their low-cost, large area, light weight, printable, and mechanical flexibility [1–5]. The properties of dielectric/semiconductor interface play an important role for charge transfer between dielectric and semiconductor, which effects electrical parameter of OFETs. Hence, treatment, using self-assembly molecules, at this interface can have dramatically improve device performance [6].

To date, several metal oxides have been investigated as dielectric layer in OFETs. Among these materials,

many studies have noticed that Al_2O_3 is an effective dielectric layer in many studies due to its controllable oxide thickness and formed high-quality self-assembled monolayers (SAMs) [7]. However, charge transport occurs in the a few nanometres between the organic semiconductor and insulator layer. It is limited because of the roughness value of Al_2O_3 and it could be increased with controlling oxidation process that is affected on device performance [8, 9]. Therefore, SAMs molecules have been examined for their ability to modify the surface properties of the Al_2O_3 insulator layer to obtain a good morphology and to form better ohmic contact. Jang et al. studied the various phosphonic acid SAMs modifying to hydrophilic surface of Al_2O_3 and compared the properties of the

Address correspondence to E-mail: tugbahanyilmaz@ktun.edu.tr

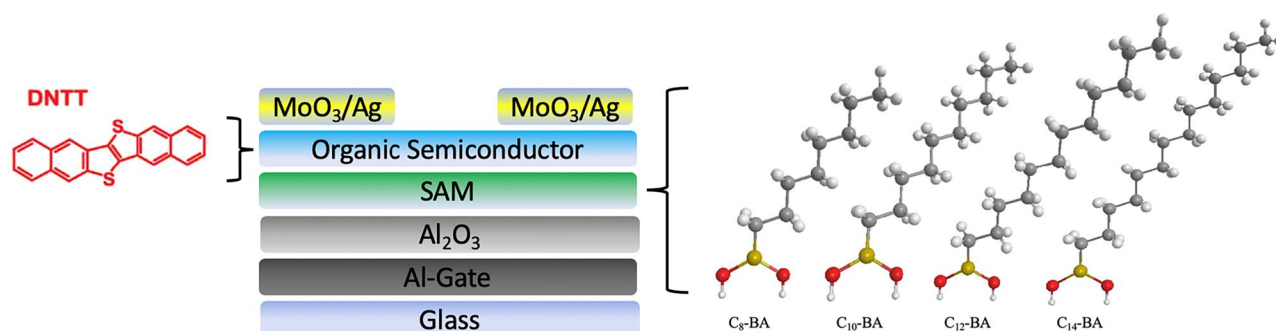


Fig. 1 Chemical structure of DNTT; schematic structure of bottom gate, top contact OFET device; chemical structures of alkyl-BA SAM molecules

SAMs according to their functional end groups and alkyl chain length [10]. The result showed that greater contact angle characteristics are produced by a surface that is more hydrophobic due to a longer alkyl chain length. The effect of gate dielectric and thickness on threshold voltage modifying with phosphonic acid-based SAMs to the Al₂O₃ surface was performed by Aghamohammadi et al. [11]. Kawanago et al. reported that the mobility and On/Off ratio increased while the trap density between Al₂O₃ gate dielectric and channel decreased after SAMs treatment [12]. These results show that the modification of SAM molecules into the Al₂O₃ dielectric layer contributes to improve the performance parameters of OFET.

Boron-based materials have been dramatically playing important role in recent years as a remarkable candidate in optoelectronic devices due to its high stability, low toxicity, easy handling, and less reactivity as well as having high quantum yield [13–16]. Organic molecules known as boronic acids are composed of a trivalent boron atom with two hydroxyl groups attached to the boron atom and one C–B bond. Boronic acids have been utilized in separation, sensing, medical therapeutics, and materials science [17–20]. In addition, the optoelectronic application of boronic acid including organic solar cells (OSCs), perovskite solar cells (PCSs), and OFET has been great attention over the last decade [21–28]. The use of boric acid derivatives in OFETs for saccharide sensing and biomolecule detection has been studied [17, 29–33]. Given that they include hydroxyl, silane, sulfonic acid, phosphonic acid, and carboxyl acid-based SAMs are the most often utilized to treat metal oxide surfaces [10, 34–37]. Addition of the potential to non-covalently mutually influence with hydrogen bonds, self-assembly of boronic acids form onto metal oxide surface shows a covalent

bond forming properties. A range of supramolecular self-assembly can develop in the solid state of boronic acids thanks to the hydroxyl groups of hydrogen bond donors [38]. Alic et al. reported that the electrical characteristics of OFETs were enhanced by using boronic acid, and its SAM molecules derivatives to treat the SiO₂ surface [39, 40]. There has been few research on alkyl-boronic acid SAM (BA-SAM) molecules, even though numerous SAM molecule types have been employed to treatment OFETs [23–25, 41]. Herein, the impact of different chain length alkyl-BA SAMs on the device performances of OFETs based on DNTT was investigated.

2 Experimental

2.1 Fabrication of OFET

As seen in Fig. 1, OFETs with a bottom-gate, top-contact configuration was fabricated on glass substrates. Dinaphtho[2,3-b:2',3'-f]thieno[3,2-b]thiophene (DNTT), an organic semiconductor based on thienoacene, was selected as the active layer because to its excellent hole mobility and air stability [42–44]. Figure 1 also displays the molecular structures of boronic acid-based SAM molecules for dielectric surface treatments for C₈-BA (*octylboronic acid*), C₁₀-BA (*decylboronic acid*), C₁₂-BA (*dodecylboronic acid*), and C₁₄-BA (*tetradecylboronic acid*). After being cleaned with organic solvents in an ultrasonic bath, the substrates were left in the UV-ozone for 10 min. Aluminum (Al) was deposited a thickness of 100 nm for the gate electrodes through a shadow mask. Thanks to the anodization process, a thin film of aluminum oxide (Al₂O₃) with a thickness of 10 nm was formed for the gate dielectric.

The anodization process detail was given in reference [45]. In short, an electrolyte solution containing citric acid was used to apply a constant current between the Pt counter electrode and the Al contact. The Al_2O_3 surface was modified by immersing the films in alkylboronic acids SAM molecules dissolved in isopropanol (IPA) (99.9%, Sigma Aldrich) at a concentration 10^{-3} M for 24 h at ambient conditions. The substrates were rinsed, dried, and then transferred in the nitrogen glove box. Afterward, a semiconducting layer of 30 nm of DNNT was deposited via thermal evaporation at a vacuum base pressure of approximately 10^{-6} mbar. A quartz crystal microbalance was used to measure the film thickness while the deposition rate was around 0.1 \AA/s . MoO_3/Ag source and drain contacts with thickness of 10 nm/60 nm were deposited using thermal evaporation, resulting in a device that had a channel length (L) of 50 μm , and a channel width (W) of 1 mm, which was utilized by the shadow mask.

2.2 Thin film and transistor characterization

The performance of organic field effect transistor fabricated is strongly integrated with the morphological, electrical, and surface characteristics of both treated and non-treated surfaces. Atomic force microscopy (AFM) is one of the most widely used methods in research for examining surface morphology. The AFM was created in response to a need to get over the constraint of Scanning Tunneling Microscopy, which can only examine conductive samples. It can examine nearly any kind of sample in a variety of environmental settings. These days, the AFM is utilized for purposes other than topographical imaging, highlighting several kinds of surface characteristics, such as the surface potential. Hence, the morphological study of both treated and non-treated substrates was performed in ambient air using an AFM (NT-MDT AFM NTEGRA Solaris) in “tapping” mode at room temperature. On the other hand, the Kelvin Probe Force Microscope (KPFM) (NT-MDT AFM NTEGRA Solaris) was used to measure the electrostatic potential of both treated and non-treated surfaces. Contact angle measurement technique is a quick and non-destructive technique to find out the hydrophobicity properties of surfaces. Since the polarity of the surface determines the contact angle, doping or adsorbing materials, such as self-assembled monolayers (SAMs), can induce modifications. Thus, to determine the hydrophobicity of the surfaces, contact angle measurement was performed.

DSA 100 KRÜSS was used to measure contact angles. The most significant characteristics of an organic field-effect transistor—charge carrier mobility, threshold voltage, subthreshold voltage, and on/off ratio—provide information on the device’s performance. To measure these properties, the OFETs were subjected to current–voltage (I – V) measurements in a nitrogen environment glovebox utilizing a 4200 Keithley semiconductor parameter analyser and a micromanipulator probe station.

3 Results and discussions

3.1 Characterization of thin films

Contact angle of water drop values were calculated onto non-treated and treated surfaces to investigate that the different chain length alkyl-BA SAMs were formed onto Al_2O_3 surfaces, As shown in Fig. 2 and As summarized in Table 1, contact angles of water were found as 63.43° on non-treated and 65.85° on C_8 -BA, 51.11° on C_{10} -BA, 55.78° on C_{12} -BA and 56.46° on C_{14} -BA SAMs treated surface.. These results are in an agreement with former studies, therein after SAMs treatment hydrophobicity decreases [46]. The C_{10} -BA (45.9 dyn/cm), C_{12} -BA (44.5 dyn/cm) and C_{14} -BA (43.9 dyn/cm) have the highest surface energy and C_8 -BA has the lowest (36.2 dyn/cm), as a comparison the surface energy of non-treated surface (38.2 dyn/cm), which indicates that more stronger surface than non-treated surface hydration occurs at the SAMs-treated surfaces [47, 48]. It also showed that could be an evidence for the dependence of the contact angle on the surface morphology [49].

In order to deprive of the surface morphology of Al_2O_3 surface and after treatment by alkyl-BA SAMs, AFM images were taken and analyzed using the WsXM software [50]. Table 1 shows measured roughness values. The surface morphology of Al_2O_3 is seen in Fig. 3 both before and after treatment. As summarized Table 1, The average roughness of surfaces increases from 1.05 nm for non-treated surface to 1.47 nm, 3.26 nm, 3.73 nm, and 2.72 nm for C_8 -BA, C_{10} -BA, C_{12} -BA, and C_{14} -BA, respectively. The findings show that the formation of alkyl-BA SAMs onto Al_2O_3 surfaces was effective to increase the average roughness of surfaces. An increase in chain length may result in a surge in all treated surfaces [51].

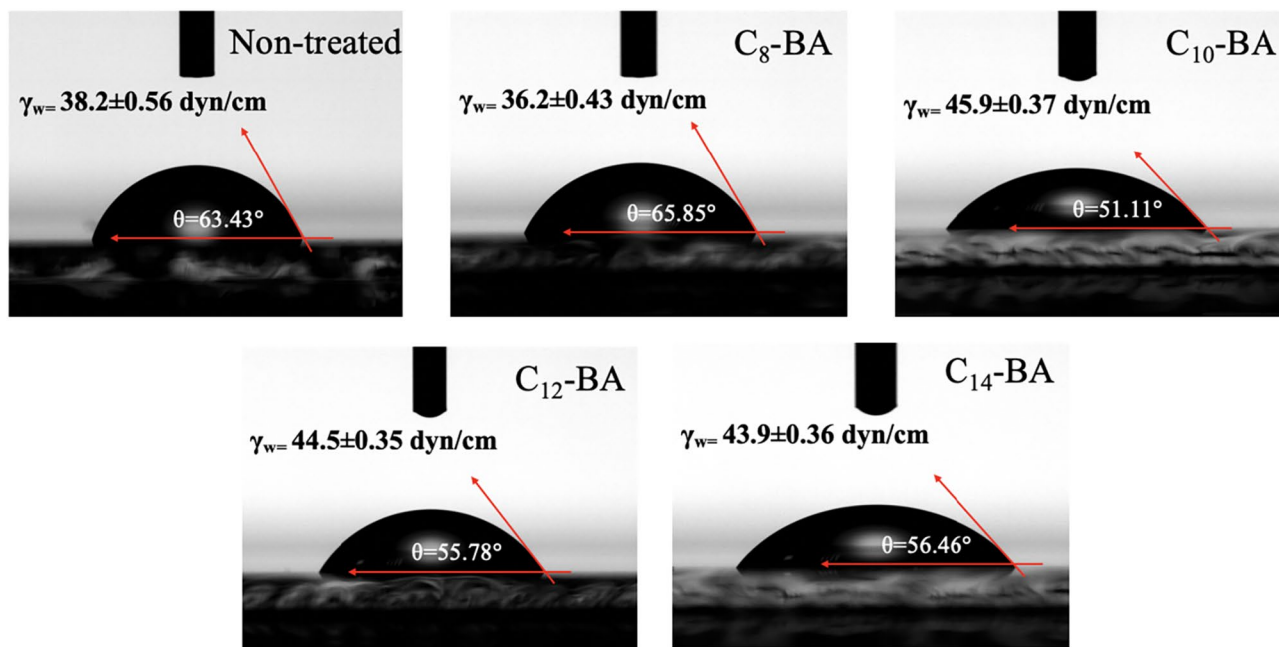


Fig. 2 Water contact angles and calculated surface tension: the surfaces of Al_2O_3 (non-treated) and treated with alkyl-BA SAM molecules

Table 1 Value of contact angle, roughness, and electrostatic potential for non-treated and boronic acids with four different chain lengths grafted Al_2O_3

	Contact angle (°)	Roughness (nm)	Roughness of DNTT layer (nm)	Electrostatic potential (V)
Non-treated	63.43	1.05	10.48	0.992
C ₈ -BA	65.85	1.41	11.55	1.033
C ₁₀ -BA	51.11	3.26	10.50	1.025
C ₁₂ -BA	55.78	3.37	13.63	1.030
C ₁₄ -BA	56.46	2.72	10.59	1.155

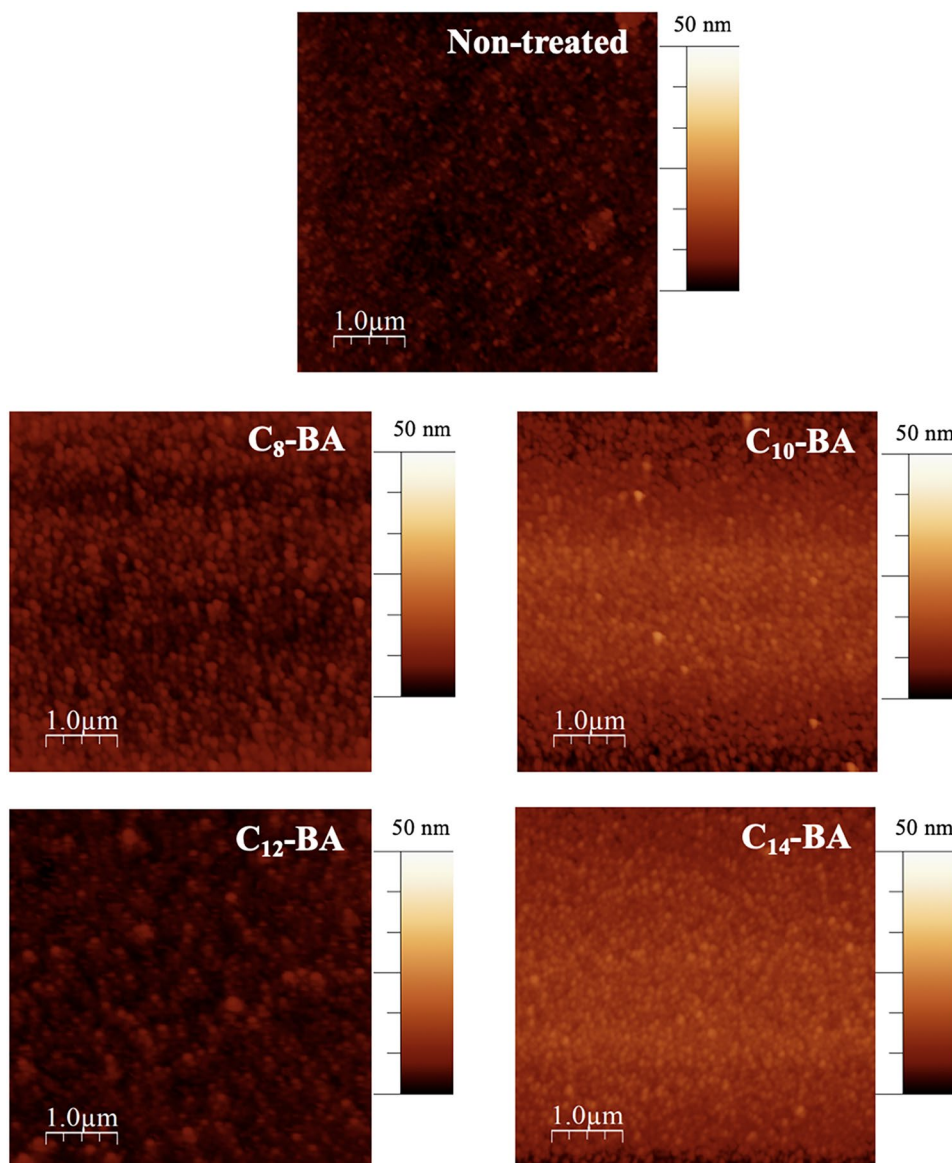
As shown Table 1, average roughness of DNTT layer onto non-treated and treated surface increased from 10.48 to 11.55 nm for C₈-BA, 10.50 nm for C₁₀-BA, 13.63 nm for C₁₂-BA, and 10.59 nm for C₁₄-BA. Furthermore, exceptionally thin DNTT layer (3 nm) was evaporated to understand behind mechanism dielectric and semiconductor layer, as shown Fig. 4. Grain sizes of DNTT is showed clearly differences which lead to effect electrical parameter of OFETs thanks to decreasing the density of charge traps [6, 52]. As seen Fig. 4, grain size of DNTT on the C₈-BA and C₁₀-BA have a grain size of $\sim 0.6 \mu\text{m}$, which is clearly bigger than on non-treated, C₁₂-BA and C₁₄-BA SAMs.

The alkyl chain length and the different SAMs have been reported for a various study such as phosphonic acid on Al_2O_3 [53], phosphonic acid on SiO_2 [54], carboxylic acid on Al_2O_3 [55], and phosphates on TiO_2

[56]. There are no studies on the relationship between the alkyl chain length and SAM structure of boronic acids on aluminum oxide. The binding mechanism between SAMs and metal oxide surface may exhibit different behavior due to SAMs microstructure. Hence, we may argue that alkyl-BA SAMs of less about ten carbon atoms could be form disordered and liquid-like monolayers which are affected the surface morphology [57].

To measure the electrostatic potential of surfaces and understand electronic interaction the non-treated and treated surfaces and the DNTT, KPFM measurements was performed [58]. As summarized in Table 1, non-treated surface shows an electrostatic potential value of 0.992 eV and treated surfaces have an electrostatic potential value of 1.033 eV, 1.025 eV, 1.03 eV, and 1.155 eV for C₈-BA, C₁₀-BA, C₁₂-BA, and C₁₄-BA

Fig. 3 Atomic force microscopy (AFM) height images of the surfaces of Al_2O_3 (non-treated) and treated with alkyl-BA SAM molecules



SAMs, respectively. Alkyl-BA SAMs do not show a wide range surface potential value for Al_2O_3 compared to phosphonic acids [11].

The charge layer, introduced by charge mobility, between non-treated/treated surface and semiconductor, is affected on electrical parameter of device [53]. In addition, the electrical properties of surfaces could also influence on morphology of following layer.

3.2 Electrical parameters of OFETs

One of main aim of this study was to investigate the effect of alkyl-BA SAMs with different chain length on OFETs performance. Figure 5 display the typical

transfer and output curves of non-treated and treated with alkyl-BA SAM OFETs. Current On/Off ratio was calculated almost 10^5 in gate voltage sweeps. Within drain voltage sweeps, proper linear and saturation behaviors were observed. The transfer curves of non-treated and treated with alkyl-BA SAM devices showed a significant difference with forward and backward scans. All the devices presented a big hysteresis effect because of impurities, defect of active layer morphology or electron trap in the insulating layer. Box charts of the electrical parameters of non-treated and treated with alkyl-BA SAM OFETs are represented comparatively (Fig. 6).

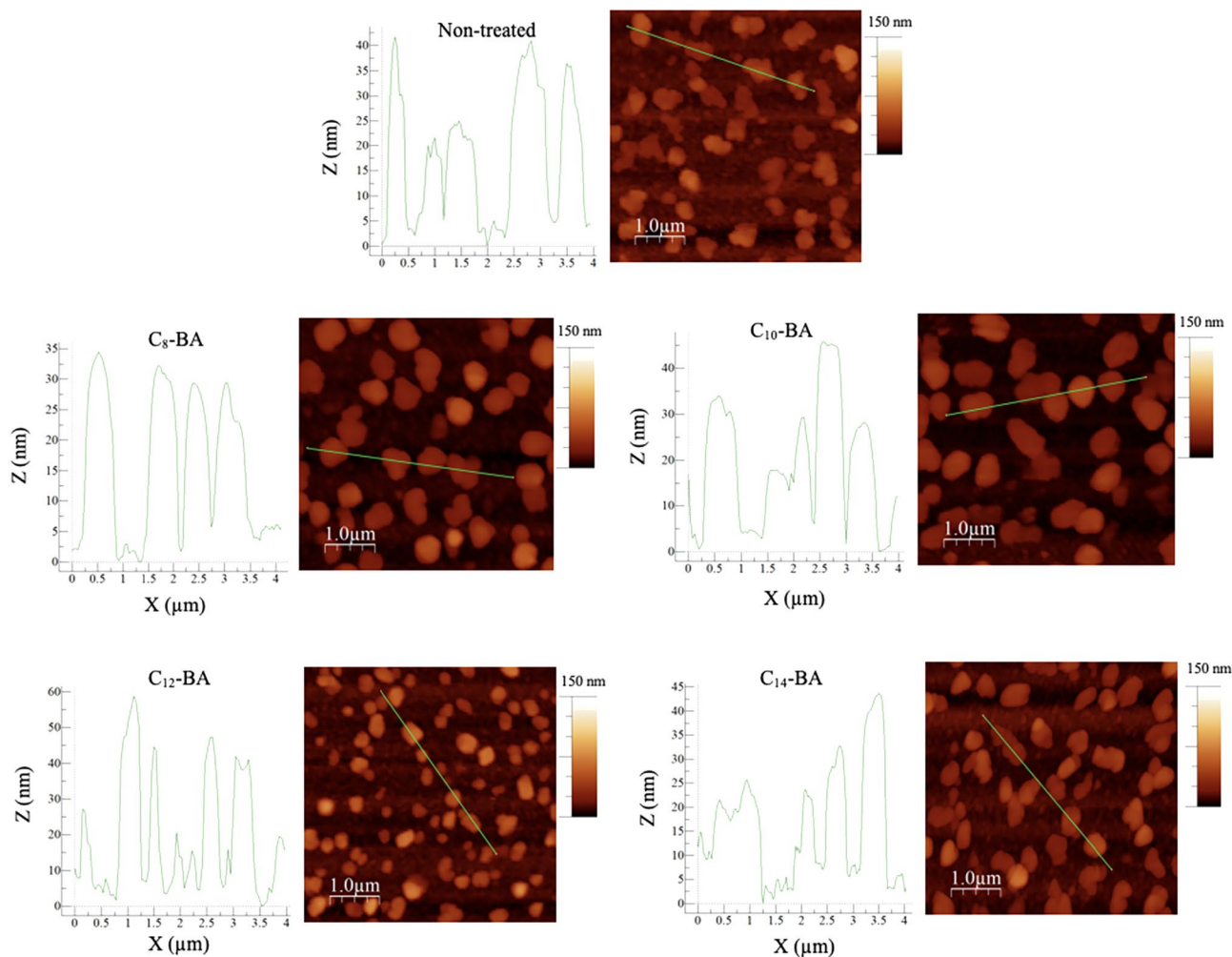


Fig. 4 Atomic force microscopy (AFM) height images of very thin layer (3 nm) of DNTT active layer on bare Al_2O_3 (non-treated) and treated surfaces. Line profiles in random direction are provided on the left of each image

The influence of treating alkyl-BA SAMs was assessed for each configuration using at least 10 OFETs. For OFETs, the linear (μ_{lin}) and saturation (μ_{sat}) mobilities were calculated using the following equations:

$$\mu_{\text{lin}} = \frac{L}{C_i W V_{ds}} \left(\frac{\partial I_{ds}}{\partial V_{gs}} \right); \mu_{\text{sat}} = \frac{2L}{C_i W} \left(\frac{\partial \sqrt{I_{ds}}}{\partial V_{gs}} \right)^2 \quad (1)$$

where L is the channel length, W is the channel width, and C_i is the dielectric capacitance. The maximum values were taken from the gate voltage dependent mobility curves. The electrical parameters of OFETs extracted from transfer curves are listed in Table 2. Although C_{10} -BA shows a similar mobilities with non-treated samples, generally Alkyl-BA SAMs treated

OFETs indicated higher mobility than non-treated samples for both regimes. Increasing the surface roughness could cause positive effect on decreasing interface trap intensity as well as negative effect on the mobilities of OFETs. Therefore, resulting in high mobilities for C_8 -BA SAM, C_{12} -BA SAM, and C_{14} -BA SAM were observed.

Threshold voltage (V_{th}) is another important parameter which is extracted from the square root of the drain current by extending the linear part to the zero current. The forward and backward scanned curves for V_{th} are also used to observed Hysteresis (ΔV_{th}) effect. Herein, notable differences were observed for Alkyl-BA SAMs treated OFETs. Threshold voltage of devices presented a decrease from around -0.52 V for non-treated device, to -0.32 V for C_8 -BA SAM, 0.10 V for

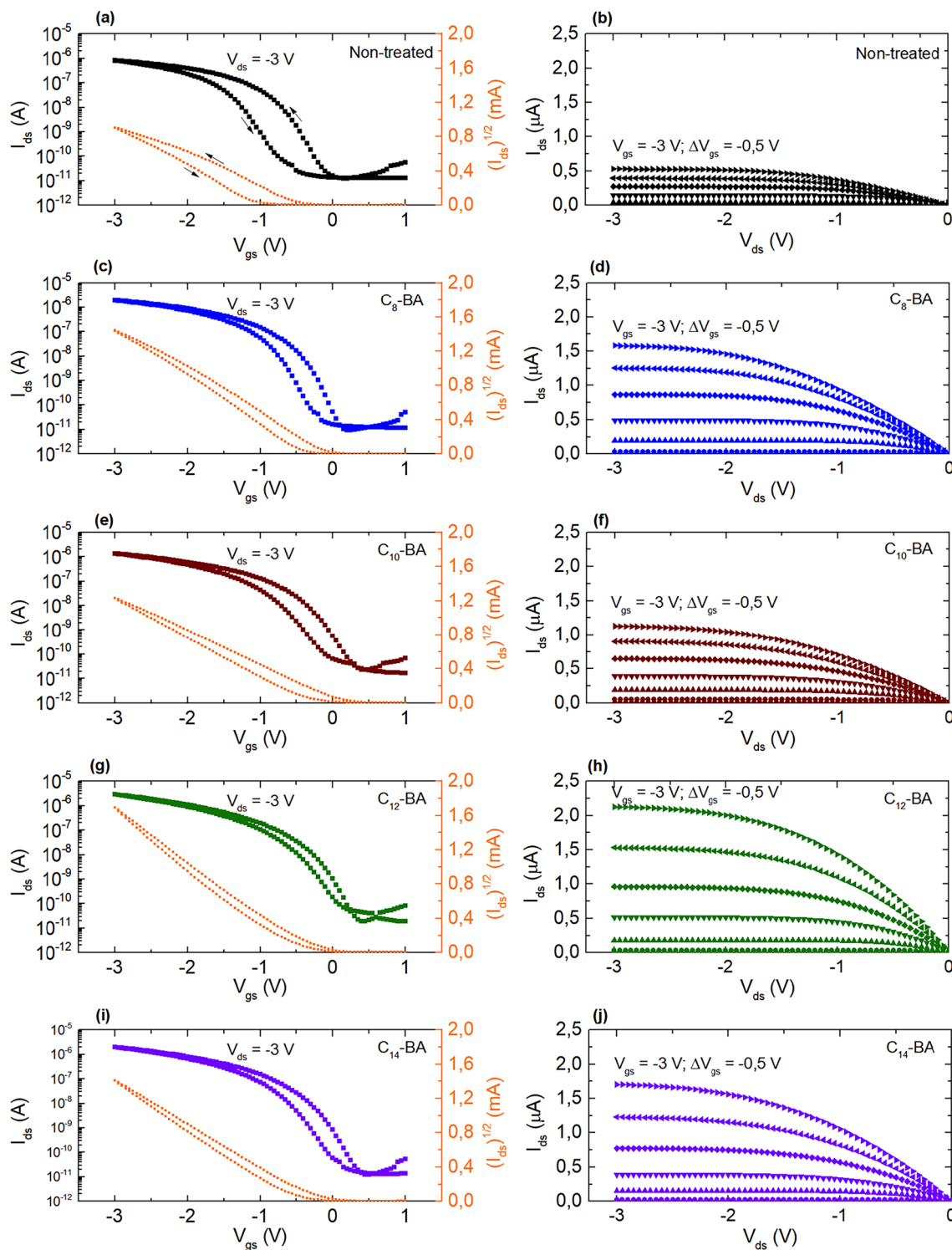
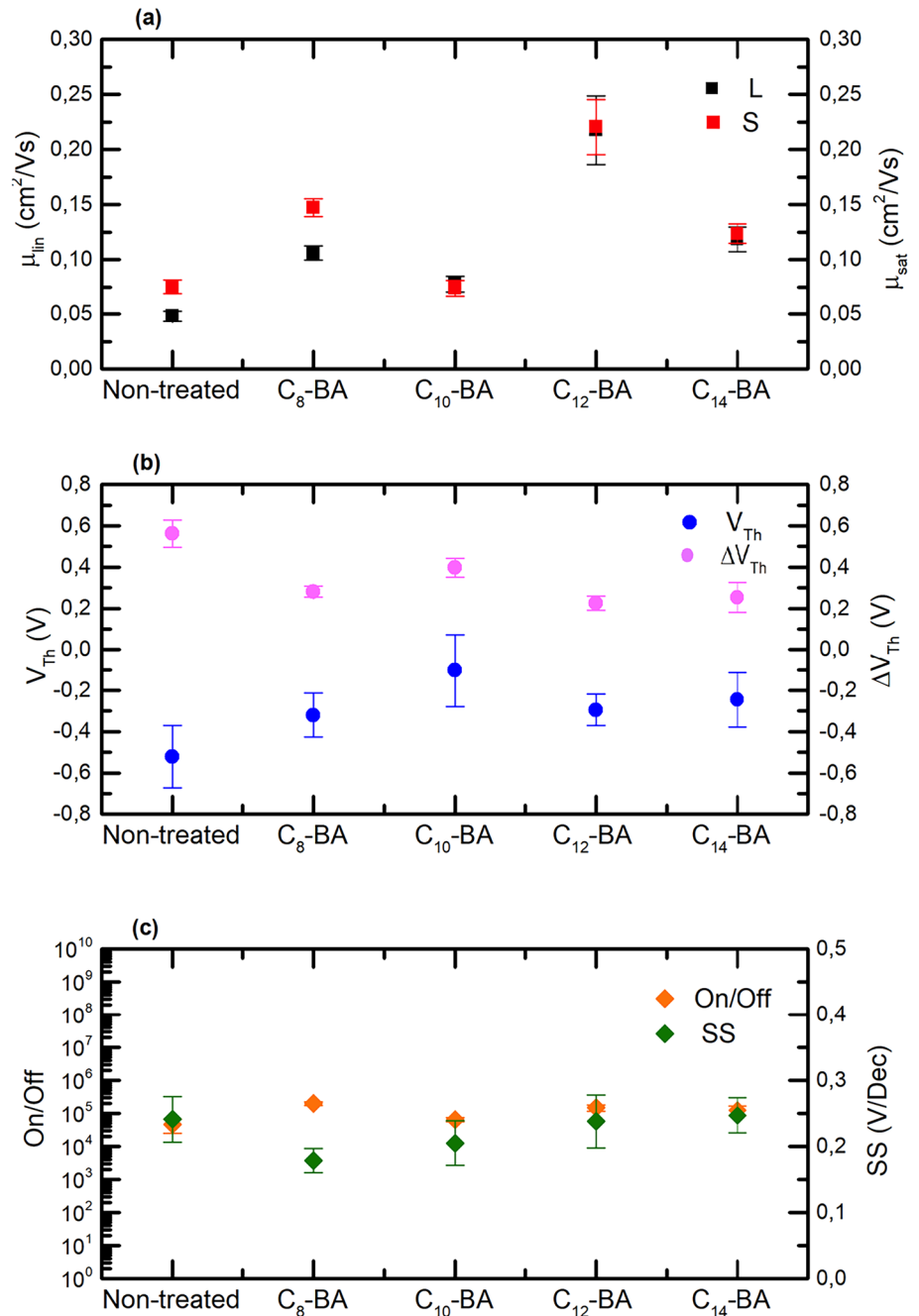


Fig. 5 Transfer (a) and output (b) characteristics of the devices on non-treated; those of the devices treated with alkyl-BA SAM molecules: C₈-BA (c) and (d); C₁₀-BA (e) and (f); C₁₂-BA (g) and (h); C₁₄-BA (i) and (j)

C₁₀-BA SAM, 0.29 V for C₁₂-BA SAM, and 0.24 V for C₁₄-BA SAM treated devices. These results also demonstrated the successful formation of alkyl-BA SAM

on Al₂O₃ surfaces. On the other hand, ΔV_{th} values also reduced from around 0.57 V in non-treated device to about 0.28 V for C₈-BA SAM, 0.39 V for C₁₀-BA SAM,

Fig. 6 Device performance parameters of OFETs with non-treated and alkyl-BA SAMs treated Al_2O_3 dielectric: linear mobility (μ_{lin}), saturation mobility (μ_{sat}), threshold voltage (V_{th}), hysteresis (ΔV_{th}), subthreshold slope (SS), and current on/off ratio ($I_{\text{on}}/I_{\text{off}}$)



0.22 V for C_{12} -BA SAM, and 0.25 V for C_{14} -BA SAM treated devices. Decreasing hysteresis effect is a powerful indication that Alkyl-BA SAM form onto the oxide surface BA SAM due to saturating charge trapping. Subthreshold slope (SS) which is associated with the interface trap densities [59], calculated as 0.18 V/dec for C_8 -BA SAM, 0.10 V/dec for C_{10} -BA SAM, 0.23 V for C_{12} -BA SAM, and 0.24 V for C_{14} -BA SAM treated devices in contrast to 0.24 V/dec for the non-treated

device. After Alkyl-BA SAM treatment, SS values also confirmed the decreasing trap densities at the interface. There were no significant differences in current on/off ratio in devices, and this showed that good gate control on devices [60].

Table 2 Summary of device performance parameters of OFETs with non-treated and boronic acids with four different chain lengths grafted Al₂O₃ dielectric

	μ_{lin} (cm ² /Vs)	μ_{sat} (cm ² /Vs)	V_{Th} (V)	ΔV_{Th} (V)	$I_{\text{On}}/I_{\text{Off}}$	SS (V/dec)
Non-treated	0.05 ± 0.004	0.08 ± 0.006	-0.52 ± 0.152	0.57 ± 0.066	0.5 × 10 ⁵	0.24 ± 0.034
C ₈ -BA	0.11 ± 0.006	0.15 ± 0.008	-0.32 ± 0.106	0.28 ± 0.023	2.1 × 10 ⁵	0.18 ± 0.018
C ₁₀ -BA	0.07 ± 0.003	0.08 ± 0.003	-0.10 ± 0.062	0.39 ± 0.046	0.7 × 10 ⁵	0.20 ± 0.034
C ₁₂ -BA	0.22 ± 0.031	0.22 ± 0.025	-0.29 ± 0.076	0.22 ± 0.033	1.5 × 10 ⁵	0.23 ± 0.040
C ₁₄ -BA	0.12 ± 0.011	0.12 ± 0.008	-0.24 ± 0.131	0.25 ± 0.072	1.3 × 10 ⁵	0.24 ± 0.026

4 Conclusion

In summary, the Al₂O₃ dielectric surface treatment with the alkyl chain lengths BA SAM molecules could enhance the electrical performance of OFETs. Nonetheless, the surface energy shows a little difference proven by water contact angle measurements, significant improvements were observed in some device performance parameters such as mobility and threshold voltage. Since these electrical parameters are related to the trap densities of the interface layer, treating alkyl chain lengths boronic acid molecules the Al₂O₃ surface is proven to be a powerful approach to passivation of the Al₂O₃ surface. In addition, the chain length of the boronic acid SAM molecules has a significant effect on the surface morphology of semiconductor and OFET performance. We observe that the medium chain length treated OFETs have the highest mobility, the largest on/off ratio, and the lowest SS value. Further developments in optoelectronics will occur because to the numerous benefits of employing SAMs, as demonstrated by a variety of examples. The following are advantages of SAM-based optoelectronic devices for future research: (1) cheap cost; (2) flexibility of the device; (3) work-function modification; and (4) increase of device stability. Because SAMs are solution processable, the SAM-based device process may be completed with straightforward spin-coating or printing, which simplifies the complexity and consequently the cost of the fabrication process. Additionally, the SAM-based process's low heat budget improves its compatibility with flexible substrates. These advantages make it very simple to deploy flexible devices such as communication devices and sensors. Therefore, this work can be pioneer a new application area associate with the boronic acid and its derivate molecules.

Author contributions

In this work, material preparation, experiments, data collection and analysis were performed by TY. The first draft of the manuscript was written by TY. The author read and approved the final manuscript.

Funding

Open access funding provided by the Scientific and Technological Research Council of Türkiye (TÜBİTAK). The author thanks Dr. Mamatimin Abbas at University of Bordeaux for their support. The author is also grateful for the financial support from the Scientific and Technological Research Council of Turkey (TÜBİTAK) (2214-A International Doctoral Research Project (PN: 1059B141501270).

Data availability

The authors declare that the datasets and results obtained and/or analyzed during the current study are available from the corresponding author on reasonable request. All data generated or analyzed during this study are included in this published article.

Declarations

Competing interests The authors declare that they have no known competing financial interests or personal relationships that could have appeared to influence the work reported in this paper.

Consent for publication The manuscript was only submitted to the journal named as "Journal of Materials Science: Materials in Electronics." The authors have certified that this manuscript was not submitted to any journal for simultaneous consideration. The au-

thors declare that the submitted results in the manuscript are original and any part of them had not been published elsewhere in any form or language (partially or in full), and this study was not split up into several parts for increasing publication number. The authors endorsed that all results introduced in this study were presented clearly, honestly, and without fabrication, falsification, or inappropriate data manipulation.

Research involving human and animal participants This study did not involve any experiments on animals or humans.

Open Access This article is licensed under a Creative Commons Attribution 4.0 International License, which permits use, sharing, adaptation, distribution and reproduction in any medium or format, as long as you give appropriate credit to the original author(s) and the source, provide a link to the Creative Commons licence, and indicate if changes were made. The images or other third party material in this article are included in the article's Creative Commons licence, unless indicated otherwise in a credit line to the material. If material is not included in the article's Creative Commons licence and your intended use is not permitted by statutory regulation or exceeds the permitted use, you will need to obtain permission directly from the copyright holder. To view a copy of this licence, visit <http://creativecommons.org/licenses/by/4.0/>.

References

1. J.A. Rogers, Z. Bao, K. Baldwin, A. Dodabalapur, B. Crone, V.R. Raju, V. Kuck, H. Katz, K. Amundson, J. Ewing, P. Drzaic, Paper-like electronic displays: large-area rubber-stamped plastic sheets of electronics and micro-encapsulated electrophoretic inks. *Proc. Natl. Acad. Sci. U.S.A.* **98**, 4835–4840 (2001)
2. T. Someya, T. Sekitani, S. Iba, Y. Kato, H. Kawaguchi, T. Sakurai, A large-area, flexible pressure sensor matrix with organic field-effect transistors for artificial skin applications. *Proc. Natl. Acad. Sci. U.S.A.* **101**, 9966 (2004)
3. S.G. Surya, H.N. Raval, R. Ahmad, P. Sonar, K.N. Salama, V.R. Rao, Organic field effect transistors (OFETs) in environmental sensing and health monitoring: a review. *TrAC Trends Anal. Chem.* **111**, 27–36 (2019)
4. Z.A. Lamport, H.F. Haneef, S. Anand, M. Waldrip, O.D. Jurchescu, Tutorial: organic field-effect transistors: materials, structure and operation. *J. Appl. Phys.* **124**, 071101 (2018)
5. W. Tang, Y. Huang, L. Han, R. Liu, Y. Su, X. Guo, F. Yan, Recent progress in printable organic field effect transistors. *J. Mater. Chem. C* **7**, 790–808 (2019)
6. S. Casalini, C.A. Bortolotti, F. Leonardi, F. Biscarini, Self-assembled monolayers in organic electronics. *Chem. Soc. Rev.* **46**, 40–71 (2017)
7. J.P. Folkers, C.B. Gorman, P.E. Laibinis, S. Buchholz, G.M. Whitesides, R.G. Nuzzo, Self-assembled monolayers of long-chain hydroxamic acids on the native oxide of metals. *Langmuir* **11**, 813–824 (1995)
8. V. Coropceanu, J. Cornil, D.A. Da Silva Filho, Y. Olivier, R. Silbey, J.L. Bredas, Charge transport in organic semiconductors. *Chem. Rev.* **107**, 926–952 (2007)
9. V. Podzorov, E. Menard, A. Borissov, V. Kiryukhin, J.A. Rogers, M.E. Gershenson, Intrinsic charge transport on the surface of organic semiconductors. *Phys. Rev. Lett.* **93**, 086602 (2004)
10. S. Jang, D. Son, S. Hwang, M. Kang, S.-K. Lee, D.-Y. Jeon, S. Bae, S.H. Lee, D.S. Lee, T.-W. Kim, Hybrid dielectrics composed of Al₂O₃ and phosphonic acid self-assembled monolayers for performance improvement in low voltage organic field effect transistors. *Nano Converg.* **5**, 20 (2018)
11. M. Aghamohammadi, R. Rödel, U. Zschieschang, C. Ocal, H. Boschker, R.T. Weitz, E. Barrena, H. Klauk, Threshold-voltage shifts in organic transistors due to self-assembled monolayers at the dielectric: evidence for electronic coupling and dipolar effects. *ACS Appl. Mater. Interfaces* **7**, 22775–22785 (2015)
12. W. Cai, J. Zhang, J. Wilson, J. Brownless, S. Park, L. Majewski, A. Song, Significant performance improvement of oxide thin-film transistors by a self-assembled monolayer treatment. *Adv Electron. Mater.* **6**, 1901421 (2020)
13. H. Lee, D. Karthik, R. Lampande, J.H. Ryu, J.H. Kwon, Recent advancement in boron-based efficient and pure blue thermally activated delayed fluorescence materials for organic light-emitting diodes. *Front. Chem.* (2020). <https://doi.org/10.3389/fchem.2020.00373>
14. U.B. Demirci, P. Miele, P.G. Yot, Boron-based (nano-) materials: fundamentals and applications. *Crystals* (2016). <https://doi.org/10.3390/cryst6090118>
15. C.D. Entwistle, T.B. Marder, Applications of three-coordinate organoboron compounds and polymers in optoelectronics. *Chem. Mater.* **16**, 4574–4585 (2004)
16. S. Møllerup, S. Wang, Boron-doped molecules for optoelectronics. *Trends Chem.* (2019). <https://doi.org/10.1016/j.trechm.2019.01.003>

17. W.L.A. Brooks, B.S. Sumerlin, Synthesis and applications of boronic acid-containing polymers: from materials to medicine. *Chem. Rev.* **116**, 1375–1397 (2016)
18. D.G. Hall, Structure, properties, and preparation of boronic acid derivatives. Overview of their reactions and applications, in *Boronic Acids: Preparation*. ed. by D.G. Hall (Wiley, Hoboken, 2006), pp.1–99
19. Y.-Y. Aung, A.N. Kristanti, H.V. Lee, M.Z. Fahmi, Boronic-acid-modified nanomaterials for biomedical applications. *ACS Omega* **6**, 17750–17765 (2021)
20. K. Lacina, P. Skládal, T.D. James, Boronic acids for sensing and other applications—a mini-review of papers published in 2013. *Chem. Cent. J.* **8**, 60 (2014)
21. Ç. Kırbıyık, M. Can, M. Kuş, Interfacial modification via boronic acid functionalized self-assembled monolayers for efficient inverted polymer solar cells. *Mater. Sci. Semicond. Process.* **107**, 104860 (2020)
22. M. Şimşek, Electro-optical properties of the perfect reflector material: poly(3-thiophene boronic acid) semiconducting polymer. *Polym. Eng. Sci. Eng. Sci.* **56**, 707–714 (2016)
23. Ç. Kırbıyık, D. Akın Kara, K. Kara, S. Büyükçelebi, M.Z. Yiğit, M. Can, M. Kuş, Improving the performance of inverted polymer solar cells through modification of compact TiO₂ layer by different boronic acid functionalized self-assembled monolayers. *Appl. Surf. Sci.* **479**, 177–184 (2019)
24. Ç. Kırbıyık, K. Kara, D.A. Kara, M.Z. Yiğit, B. İstanbullu, M. Can, N.S. Sarıçiftci, M. Scharber, M. Kuş, Enhancing the c-TiO₂ based perovskite solar cell performance via modification by a serial of boronic acid derivative self-assembled monolayers. *Appl. Surf. Sci.* **423**, 521–527 (2017)
25. Ç. Kırbıyık, T. Yılmaz Alıç, M. Kuş, Influence of alkyl chain length of boronic acid self-assembled monolayers on indium tin oxide and their organic solar cell performance. *Microelectron. Eng.* **231**, 111394 (2020)
26. Ç. KırbıyıkKurukavak, T. Yılmaz, A. Büyükbekar, M. Kuş, Surface modification of c-TiO₂ via different phenyl boronic acid SAMs for improved performance of inverted organic solar cells. *Mater. Sci. Semicond. Process.* **135**, 106120 (2021)
27. Ç. KırbıyıkKurukavak, T. Yılmaz, A. Büyükbekar, M. Kuş, Effect of different terminal groups of phenyl boronic acid self-assembled monolayers on the photovoltaic performance of organic solar cells. *Opt. Mater.* **112**, 110783 (2021)
28. T. Yılmaz, Ç. KırbıyıkKurukavak, Comparison of self-assembled monolayers with long alkyl chains on ITO for enhanced surface properties and photovoltaic performance. *Opt Quantum Electron.* **53**, 170 (2021)
29. J.-I. Anzai, Recent progress in electrochemical biosensors based on phenylboronic acid and derivatives. *Mater. Sci. Eng. C* **67**, 737–746 (2016)
30. Y. Egawa, T. Seki, S. Takahashi, J.-I. Anzai, Electrochemical and optical sugar sensors based on phenylboronic acid and its derivatives. *Mater. Sci. Eng. C* **31**, 1257–1264 (2011)
31. A. Matsumoto, H. Matsumoto, Y. Maeda, Y. Miyahara, Simple and robust strategy for potentiometric detection of glucose using fluorinated phenylboronic acid self-assembled monolayer. *Biochim. et Biophys. Acta (BBA)—Gen. Subj.* **1830**, 4359–4364 (2013)
32. A. Matsumoto, N. Sato, T. Sakata, K. Kataoka, Y. Miyahara, Glucose-sensitive field effect transistor using totally synthetic compounds. *J. Solid State Electrochem. Electrochem.* **13**, 165–170 (2009)
33. S. Takahashi, J.-I. Anzai, Phenylboronic acid monolayer-modified electrodes sensitive to sugars. *Langmuir* **21**, 5102–5107 (2005)
34. K. Amer, S. Ebrahim, M. Feteha, M. Soliman, A. Mohamed Elshaer, *Organic field effect transistor based on polyaniline—dodecylbenzene sulphonic acid for humidity sensor*, 34th National Radio Science Conference (NRSC), (2017), pp. 440–447
35. M. Singh, N. Kaur, E. Comini, The role of self-assembled monolayers in electronic devices. *J. Mater. Chem. C* **8**, 3938–3955 (2020)
36. H. Ma, O. Acton, D.O. Hutchins, N. Cernetic, A.K.Y. Jen, Multifunctional phosphonic acid self-assembled monolayers on metal oxides as dielectrics, interface modification layers and semiconductors for low-voltage high-performance organic field-effect transistors. *Phys. Chem. Chem. Phys.* **14**, 14110–14126 (2012)
37. S. Jadhav, Self-assembled monolayers (SAMs) of carboxylic acids: an overview. *Cent. Eur. J. Chem.* **9**, 369–378 (2011)
38. R. Nishiyabu, Y. Kubo, T.D. James, J.S. Fossey, Boronic acid building blocks: tools for self assembly. *Chem. Commun. Commun.* **47**, 1124–1150 (2011)
39. T.Y. Alıç, A. Ablat, A. Kyndiah, Y. Nicolas, M. Can, M. Kuş, M. Abbas, Interface modification of DNTT-based organic field effect transistors using boronic acid derivatives. *J. Phys. D Appl. Phys.* **53**, 065108 (2019)
40. T. Yılmaz Alıç, The effect of phenylboronic acid-based self-assembled monolayers on the performance of organic field-effect transistors (OFETs). *Turk. J. Phys.* **43**, 207–212 (2019)

41. D. Akin Kara, K. Kara, G. Oylumluoglu, M.Z. Yigit, M. Can, J.J. Kim, E.K. Burnett, D.L. Gonzalez Arellano, S. Buyukcelebi, F. Ozel, O. Usluer, A.L. Briseno, M. Kus, Enhanced device efficiency and long-term stability via boronic acid-based self-assembled monolayer modification of indium tin oxide in a planar perovskite solar cell. *ACS Appl. Mater. Interfaces* **10**, 30000–30007 (2018)
42. T. Yamamoto, K. Takimiya, Facile synthesis of highly π -extended heteroarenes, dinaphtho[2,3-b:2',3'-f]chalcogenopheno[3,2-b]chalcogenophenes, and their application to field-effect transistors. *J. Am. Chem. Soc.* **129**, 2224–2225 (2007)
43. U. Zschieschang, F. Ante, D. Kälblein, T. Yamamoto, K. Takimiya, H. Kuwabara, M. Ikeda, T. Sekitani, T. Someya, J.B. Nimoth, H. Klauk, Dinaphtho[2,3-b:2',3'-f]thieno[3,2-b]thiophene (DNTT) thin-film transistors with improved performance and stability. *Org. Electron.* **12**, 1370–1375 (2011)
44. U. Zschieschang, F. Ante, T. Yamamoto, K. Takimiya, H. Kuwabara, M. Ikeda, T. Sekitani, T. Someya, K. Kern, H. Klauk, Flexible low-voltage organic transistors and circuits based on a high-mobility organic semiconductor with good air stability. *Adv. Mater.* **22**, 982–985 (2010)
45. M. Abbas, G. Cakmak, N. Tekin, A. Kara, H. Yuksel-Guney, E. Arici, N. SerdarSariciftci, Water soluble poly(1-vinyl-1,2,4-triazole) as novel dielectric layer for organic field effect transistors. *Org. Electron. Mar.* **12**(3), 497–503 (2011)
46. T. Watanabe, Wettability of ceramic surfaces—a wide range control of surface wettability from super hydrophilicity to super hydrophobicity, from static wettability to dynamic wettability. *J. Ceram. Soc. Jpn.Jpn.* **117**, 1285–1292 (2009)
47. G.D. Davis, Surface treatments of selected materials, in *Handbook of Adhesion Technology*. ed. by L.F.M. da Silva, A. Öchsner, R.D. Adams (Springer, Heidelberg, 2017), pp.1–33
48. J. Wang, Z. Kan, F. Wang, W. Zheng, Improving frictional properties of DLC films by surface energy manipulation. *RSC Adv.* **8**, 11388–11394 (2018)
49. S.J. Hitchcock, N.T. Carroll, M.G. Nicholas, Some effects of substrate roughness on wettability. *J. Mater. Sci.* **16**, 714–732 (1981)
50. I. Horcas, R. Fernández, J.M. Gómez-Rodríguez, J. Colchero, J. Gómez-Herrero, A.M. Baro, WSXM: a software for scanning probe microscopy and a tool for nanotechnology. *Rev. Sci. Instrum.* **78**, 013705 (2007)
51. L. Fumagalli, D. Natali, M. Sampietro, E. Peron, F. Perissinotti, G. Tallarida, S. Ferrari, Al_2O_3 as gate dielectric for organic transistors: charge transport phenomena in poly-(3-hexylthiophene) based devices. *Org. Electron.* **9**, 198–208 (2008)
52. Z. Ding, G. Abbas, H.E. Assender, J.J. Morrison, S.G. Yeates, E.R. Patchett, D.M. Taylor, Effect of oxygen, moisture and illumination on the stability and reliability of dinaphtho[2,3-b:2',3'-f]thieno[3,2-b]thiophene (DNTT) OTFTs during operation and storage. *ACS Appl. Mater. Interfaces* **6**, 15224–15231 (2014)
53. M. Salinas, C.M. Jäger, A.Y. Amin, P.O. Dral, T. Meyer-Friedrichsen, A. Hirsch, T. Clark, M. Halik, The relationship between threshold voltage and dipolar character of self-assembled monolayers in organic thin-film transistors. *J. Am. Chem. Soc.* **134**, 12648–12652 (2012)
54. I.G. Hill, C.M. Weinert, L. Kreplak, B.P. van Zyl, Influence of self-assembled monolayer chain length on modified gate dielectric pentacene thin-film transistors. *Appl. Phys. A* **95**, 81–87 (2009)
55. Y.T. Tao, Structural comparison of self-assembled monolayers of n-alkanoic acids on the surfaces of silver, copper, and aluminum. *J. Am. Chem. Soc.* **115**, 4350–4358 (1993)
56. D.M. Spori, N.V. Venkataraman, S.G.P. Tosatti, F. Durmaz, N.D. Spencer, S. Zürcher, Influence of alkyl chain length on phosphate self-assembled monolayers. *Langmuir* **23**, 8053–8060 (2007)
57. K. Fukuda, T. Hamamoto, T. Yokota, T. Sekitani, U. Zschieschang, H. Klauk, T. Someya, Effects of the alkyl chain length in phosphonic acid self-assembled monolayer gate dielectrics on the performance and stability of low-voltage organic thin-film transistors. *Appl. Phys. Lett.* **95**, 203301 (2009)
58. G. Heimel, F. Rissner, E. Zojer, Modeling the electronic properties of π -conjugated self-assembled monolayers. *Adv. Mater.* **22**, 2494–2513 (2010)
59. Y. Kwon, B. Park, Subthreshold slope as a measure of interfacial trap density in pentacene films. *Thin Solid Films* **599**, 145–150 (2016)
60. Y.C. Eng, L. Hu, T.F. Chang, C.Y. Wang, S. Hsu, O. Cheng, C.T. Lin, Y.S. Lin, Z.J. Tsai, C.W. Yang, J. Lu, S.Y.W. Chen, Significance of overdrive voltage in the analysis of short-channel behaviors of n-FinFET devices. *IEEE J. Electron Devices Soc.* **10**, 281–288 (2022)

Publisher's Note Springer Nature remains neutral with regard to jurisdictional claims in published maps and institutional affiliations.